Available online at www.sciencedirect.com

SciVerse ScienceDirect

Proceedings of the Combustion Institute 34 (2013) 3145–3153

Proceedings of the Combustion Institute

www.elsevier.com/locate/proci

Acoustic characterization of a partially-premixed gas turbine model combustor: Syngas and hydrocarbon fuel comparisons

Patton M. Allison *, James F. Driscoll, Matthias Ihme

Department of Aerospace Engineering, University of Michigan, Ann Arbor, MI 48109, USA

Available online 24 July 2012

Abstract

In this work, the acoustic behavior of a combustion instability in a gas turbine model combustor was investigated as fuel properties, air flow rates, and burner geometry were varied. The dual-swirl burner, developed at DLR Stuttgart by Meier, was operated using syngas (H_2/CO), ethylene, propane, and methane. The frequency of the instability was found to vary significantly from 250 to 480 Hz. When the plenum volume and the exhaust pipe length and diameter were changed, the frequencies followed trends similar to a Helmholtz resonator. The variation of fuel type, flame speed, and air flow rate greatly altered the instability frequency and amplitude. These effects are not predicted by Helmholtz or organ tone acoustic theory. Higher frequencies were correlated with larger laminar burning velocities and higher air flow rates. The burner is a forced resonator, in which the flame oscillations couple with the flowfield to create convectively altered Helmholtz resonances. This suggests the need for an improved model of a forced Helmholtz resonator that includes flame properties. Alkane fuels displayed similar acoustic trends, but ethylene varied greatly from methane and propane. Syngas displayed different behavior than hydrocarbon fuels, even when the laminar flame speeds of the fuels were matched between ethylene and a syngas mixture. Flame characteristics such as anchoring, liftoff height, and shape appear to play a major role in the determination of instability strength and presence. With increasing hydrogen-content in the syngas-mixture, the flame transitions from a lifted to a fully anchored flame, resulting in a drastic decrease in the acoustic amplitude associated with non-resonating flames. Rayleigh indices show that flat flames create strong regions of thermo-acoustic coupling compared to axially extended V-shape flames. It is concluded that, in the current burner configuration, integrated-acoustics occur that involve a combination of Helmholtz and convective-mechanisms.

Keywords: Helmholtz; Instability; Gas turbine; Syngas; Convective–acoustic

1. Introduction

Combustion instabilities in gas turbine engines often give rise to acoustic resonances, which occur as manifestations of different acoustic modes, of which multiple modes may be present. Swirl flames impart a vital fluid-mechanical effect

* Corresponding author. Address: Department of Aerospace Engineering, University of Michigan, 1320 Beal Ave., Ann Arbor, MI 48109, USA.
E-mail addresses: pallison@umich.edu (P.M. Allison), patton.allison@gmail.com (P.M. Allison).

1540-7489/$ - see front matter © 2012 The Combustion Institute. Published by Elsevier Inc. All rights reserved.
http://dx.doi.org/10.1016/j.proci.2012.06.157

conducive to flame stabilization through creation of a central recirculation zone, enhanced mixing, and the formation of a precessing vortex core (PVC) [1]. Swirl flames are also subject to thermoacoustic oscillations that can lead to acoustic instabilities. These instabilities arise when there is sufficient in-phase coupling between the pressure field and heat release to satisfy the Rayleigh criterion [2]. Oscillations in the heat release rate can occur in different ways. The flame base may remain attached (as with fully premixed flames) and flame length oscillates. In other situations the flame base is lifted and oscillates, leading to flame area fluctuations.

This paper focuses on a dual-swirl burner that undergoes a natural combustion instability at a frequency in the range between 250 and 480 Hz. The swirl burner, known as the gas turbine model combustor (GTMC), was developed by Meier and colleagues at DLR Stuttgart. It has the advantage that it is of canonical axisymmetric swirler-design yet it exhibits the fundamental physics associated with gas turbine flames; it contains two swirling air streams which surround an annular fuel stream. Comprehensive measurements have been conducted in the burner-facility by Meier and coworkers [3,4] to investigate flame-structure, flame-dynamics, and flow-field structures for a few selected methane-fueled conditions. In the present work, the burner was operated on several syngas mixtures, propane, methane, and ethylene which have very different flame speeds and molecular weights. There have been many previous studies of combustion instabilities, but the role of the laminar burning velocity has not been investigated. Synfuels (consisting of hydrogen and carbon monoxide) are of interest for use in gas turbine combustors; they can have large burning velocities. Burning velocity is known to play a major role in determining the liftoff location and the geometry of the flame base.

The new aspects of the present work are the following. The equivalence ratio (φ), air mass flow rate (m_a), and hydrogen content were systematically varied, which results in changes in laminar burning velocity, and then the frequency and amplitude of the combustion instability were measured. Syngas flames were compared to conventional hydrocarbon cases. This paper reports significant differences associated with syngas. When the flame speeds were matched between one syngas mixture to that of ethylene, the syngas results displayed a similar frequency response, but the amplitude and flame shape differed greatly. The frequency was also found to be proportional to the flow velocity, due to a convective–acoustic mechanism.

Even with the simplest types of swirl flame geometries, it is known that several types of combustion instabilities can occur simultaneously [5,6]. Rockwell [7] has shown that when air flows over a cavity, tones occur at low frequencies that are proportional to the gas velocity, and not the acoustic velocity. Convective–acoustic modes [8,9] characterize an acoustic coupling between the flow velocity and a convected entropy wave. Lieuwen describes this wave as one that propagates downstream to some flow constriction; a new wave then is excited which moves upstream and impinges on the injector nozzle. Yu et al. systematically varied the combustor length and inlet velocity to show that the convection time for the reflected entropy wave explains their acoustic measurements.

A Helmholtz instability was identified in an industrial swirl burner by Zähringer et al. [10]. Two mechanisms were present; one controlled by the swirler geometry and one controlled by Helmholtz resonances due to the geometries of the chamber and exhaust pipe. Two independent mechanisms were observed by Samaniego et al. [11] in a premixed propane-fired dump combustor when it was operated fuel-rich or fuel-lean. The dual-mode behavior of this burner was shown to be mass flow dependent and affected by fluid-mechanical oscillations of the injected streams impinging upon each other, which creates a switching effect. Dhanuka et al. [12] studied a large-scale LPP burner operated on Jet-A fuel; they found that the frequency of their lean-limit instability was proportional to their laminar burning velocity, which was increased by raising the air preheat temperature. Steinberg et al. [13] have shown that the motion of the PVC along with the size of recirculation zones can act as a blockage to the flow and affect the flame position. The recirculation zone can change size and location, which leads to oscillations in equivalence ratio and air flow rate.

Syngas is one of the focal points of the present work. Previous syngas studies, by Lieuwen et al. [14], Fritz et al. [15], and Tuncer et al. [16] of swirl flames have measured the flame blowout limits but not the acoustics. The enhanced blowout limits were attributed to higher flame speeds afforded by the hydrogen component of syngas. This leads to smaller liftoff heights due to better flame anchoring. Syngas flames also exhibit different flame shapes than hydrocarbon flames, which result in varying amplification of instabilities.

2. Experimental apparatus

The gas turbine model combustor (GTMC) [4], shown in Fig. 1, is used to study the combustion instability. The injector consists of a central air nozzle, an annular fuel nozzle, and a co-annular air nozzle. Both air nozzles supply swirling air at atmospheric pressure and temperature from a common plenum. The inner air nozzle has a diameter of 15 mm; the annular nozzle has an inner

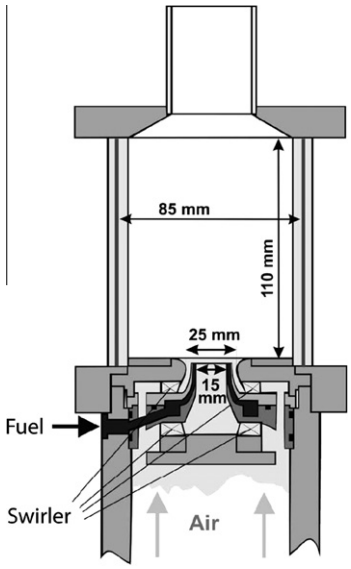

Fig. 1. The gas turbine model combustor designed by Meier et al. [4].

diameter of 17 mm and an outer diameter of 25 mm. The measured swirl number is 0.55. Non-swirling fuel is provided through three exterior ports fed through the annular nozzle which is subdivided into 72 0.5 mm × 0.5 mm channels. The exit plane of the central air nozzle and fuel nozzle lies 4.5 mm below the exit plane of the outer air annulus. Although there is no premixing within the injector, the recession of the injector facilitates partial-premixing of the reactants in the region upstream of the flame prior to combustion [17]. The degree of premixedness is a function of the liftoff height and swirling velocity.

The combustion chamber has a square cross-section of 85 mm in width and 110 mm in height. The exit of the combustion chamber is an exhaust tube with a diameter of 40 mm and a height of 50 mm. Mass flow rates for the air and individual fuel lines leading to the burner were controlled by choked orifices. The reported equivalence ratios are accurate to within ±2.25%. Table 1 lists the operating parameters investigated. The hydrocarbon fuels and syngas mixtures of 20% and 25% hydrogen by volume were burned over a range of equivalence ratios and air mass flow rates. Ethylene was chosen because its flame speed [18] over the range $\varphi = 0.65$–1.0 closely matches that of the syngas mixture of 25% H_2. In addition, ethylene also matches the flame speed [19] of the 20% H_2 mixture from $\varphi = 1.1$–1.2. Syngas gas mixtures of 10–45% hydrogen were only burned at an air mass flow rate of 282 g/min for a smaller range of equivalence ratios to study stability limits.

A PCB piezoelectric transducer was mounted in the plenum, which has a diameter of 80 mm and a length of 72 mm. For a given operating condition, pressure measurements are taken at a set burner reference temperature. The frequency and amplitude in the plenum was previously shown to be not significantly different from that in the combustion chamber, with the exception of a phase shift [20]. The reported frequencies are accurate to ±0.5% and the calculated amplitude is accurate to ±3%.

3. Results and discussion

3.1. Pressure spectrum and Helmholtz resonance

The GTMC generally operates in two different acoustic regimes: (1) acoustically resonating or (2) acoustically non-resonating. An acoustically resonating flame is defined as having a pressure fluctuation, P'_{RMS}, that is at least double that of the non-reacting cold-flow case. The results provided in this paper will focus on acoustically resonating flames and flames that abruptly transition to non-resonating cases. For all flames studied, a single resonant peak was typically present in the pressure power spectrum, as seen in Fig. 2.

When the dimensions of the GTMC combustion chamber, exhaust tube, and plenum were varied to investigate Helmholtz behavior, as described in Eq. (1), the measured frequencies followed Helmholtz-like trends. In Eq. (1), the resonant frequency is given by f_o, whereas c represents the speed of sound, A and L correspond to the

Table 1
Fueling parameters investigated.

Fuel	m_a (g/min)	Φ_{Global}	S_L ($\Phi = 1$) (cm/s)
Syngas, H_2/CO vol.%			
20% H_2	170–354	0.75–1.2	60
25% H_2	170–354	0.65–1.1	68
10–45% H_2	282	0.75–1.1	35–105
Methane	170–354	0.65–1.2	40
Propane	170–354	0.65–1.2	44
Ethylene	170–354	0.65–1.2	65

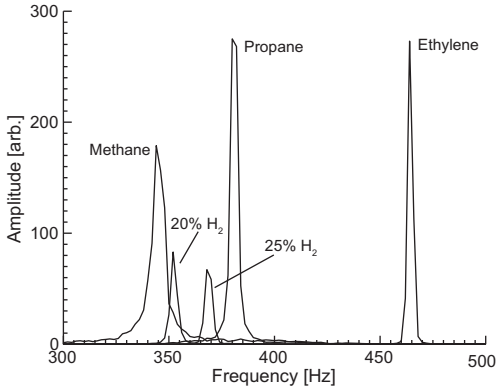

Fig. 2. Pressure power spectrum for the various fuels studied at $\varphi = 1$.

resonator neck area and length, and V corresponds to the resonator volume. Table 2 summarizes the dimensions varied and the percent change from the nominal frequency of 320 Hz for a propane flame operated at $\varphi = 0.75$ and $m_a = 282$ g/min, for the standard burner configuration. When the combustion chamber length was varied from 75 to 300 mm, no frequency shift larger than 5% was observed. This result indicates no acoustic mode, which scales with combustor length, is present. As well, since a single resonant peak is observed, the plenum and combustor are acoustically coupled. Changes to the volume of the plenum indicate a Helmholtz resonance is associated with its dimensions, as there was a 28% frequency change. Steinberg et al. [21] observed that a bulk mode oscillation is present since pressures measured at several locations in the combustor were in phase, and had a 60° phase shift between the plenum and combustor.

$$f_0 = \frac{c}{2\pi}\sqrt{\frac{A_{\text{Neck}}}{L_{\text{Neck}} \cdot V}} \tag{1}$$

The largest frequency changes were observed in changes involving the exhaust tube. Increasing the tube length by a factor of 10 caused the frequency to shift by 125 Hz to lower frequencies.

Table 2
GTMC configurations investigated for propane fuel at $\varphi = 0.75$ and $m_a = 282$ g/min.

Component	Variation	Frequency change (% change from 320 Hz)
Chamber		
Length	32% to +270%	<5
Exhaust tube		
Length	+975%	−39
Diameter	−67%	−35
Plenum		
Volume	+400%	−28

Changing the diameter of the exhaust pipe resulted in a smaller change to the frequency, but a large increase in the amplitude of the instability was observed. The geometry of the GTMC is representative of two Helmholtz resonators in series. The swirler and exhaust tube may respectively act as necks for the plenum and combustor. If a lumped-acoustic model [22] for a Helmholtz resonator is considered, the results suggest that the exhaust pipe length and diameter play a role in changing the impedance of the system. The data shown in Fig. 3 represent all the variations of plenum volume, exhaust length, and exhaust diameter conducted for a propane flame operated at $\varphi = 0.75$ and $m_a = 282$ g/min. While the data qualitatively follows Helmholtz-like trends, the correct dimensional scalings are not observed. For example, when the length of the 40 mm diameter exhaust tube is increased, the frequency scales with $L_{\text{Exhaust}}^{-0.26}$; whereas the expected scaling is $L_{\text{Exhaust}}^{-1/2}$. As well, the variation of plenum volume does not follow an expected scaling of $V_{\text{Plenum}}^{-1/2}$.

The data in Fig. 3 suggest that a Helmholtz-type resonance occurs and that coupling exists between the acoustics and fluid-flame motions, which is consistent with the ideas proposed by Steinberg et al. [21]. Thus, the resonant frequency and amplitude are altered by the flame, the flow pattern, and the geometry of the burner. In a pure Helmholtz resonator, the motion of a fluid element in the neck causes an isentropic compression of the volume of fluid in the plenum, which may be violated in the presence of a flame and a complex separated flow pattern. Previous acoustic resonator studies have reported that the resonant frequency is altered by the flow velocity and burning velocity [23–25]. The length scales varied in this study may not be sufficient to model the Helmholtz behavior of the GTMC. Rather, the coupling between the acoustics and flame may introduce new "effective" length scales [26], which are related to the discussed dimensions.

3.2. Comparison of syngas and hydrocarbon fuels: laminar flame speed effects

Helmholtz resonator theory may explain the frequency variations observed with dimensional changes, however, it is unable to capture influences due to the presence of a flame. Laminar flame speeds were varied by changing both fuel type and global equivalence ratio, φ. Once the gases leave the injector, there will be some degree of premixing over the liftoff height. Figure 4a shows the measured frequency response of the pressure oscillation with varying equivalence ratio. The frequency response generally increases with equivalence ratio, except for alkanes which show non-monotonic trends. The highest frequencies occur for the fastest burning fuels (ethylene and syngas) and the maximum values tend to

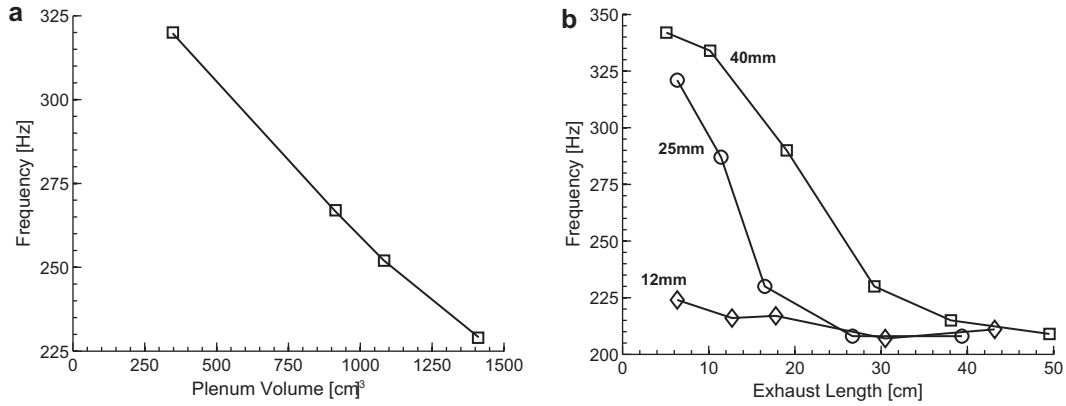

Fig. 3. Frequency response to burner configuration variations. (a) Effect of varying plenum volume; (b) effect of varying exhaust tube length with various tube diameters; 40 mm, 25 mm, and 12 mm.

occur for stoichiometric or slightly rich conditions.

Figure 4b shows the relationship between the observed frequency and the flame speed of a given mixture at all studied equivalence ratios for $m_a = 282$ g/min. Flame speed data for propane and methane were acquired from Yu [27]. The frequency of the instability is nearly linearly

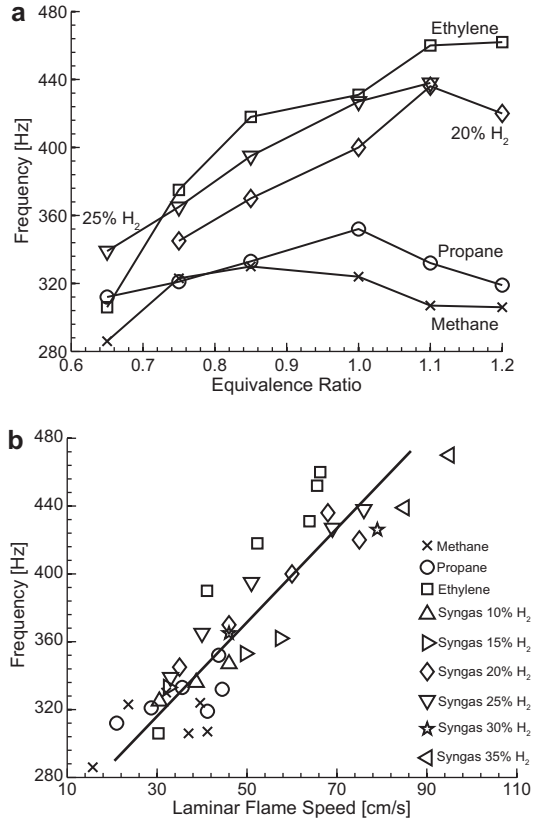

Fig. 4. Effect of laminar burning velocity on the frequency of the combustion instability. (a) Effect of equivalence ratio at $m_a = 282$ g/min; (b) frequency as a function of flame speed for all fuels studied at $m_a = 282$ g/min, for varying $\varphi = 0.65$–1.2.

proportional to the laminar burning velocity for a wide range of fuels and equivalence ratios. This result is unexpected and not explained by conventional acoustic concepts. The presence of a flame in a Helmholtz resonator creates a driven state. Helmholtz theory describes a fluid element in the "neck" region which oscillates as a simple harmonic oscillator. This oscillation can be altered by the flame as it is swept downstream and then propagates rapidly upstream, a motion dependent on the laminar burning velocity. Other possible explanations are that the burning velocity affects the flame base liftoff height and the flame shape, both of which may influence the acoustic impedance.

It is noted that the adiabatic flame temperature also changes as the fuel type and equivalence ratio are varied, and this can change the speed of sound of the product gases. However, the variation in temperature is not large enough to explain the significant variation in frequencies observed.

3.3. Mean flow velocity variation

Instabilities that are of a convective–acoustic type display a frequency that varies with the gas velocity, while those that are pure Helmholtz types do not. To investigate these effects the air mass flow rate was varied. Figure 5 indicates that the frequency of the instability increases with increasing air mass flow rate. This suggests that the instability depends on a Strouhal number [24] and has a convective–acoustic component. Oscillations in heat release and pressure are caused by rapid changes in flame location, shape, liftoff height. These perturbations are propagated back to the injector nozzle where a perturbation is induced in the fuel and air streams, resulting in perceived equivalence ratio oscillations. These equivalence ratio oscillations are convected to the flame at a speed proportional to the mean flow velocity, which perpetuates the evolution of fluctuations in flame properties, such as heat release. The frequency data in Fig. 5 are similar for the syngas (25% H_2) and ethylene, which have the same flame speeds. The relationship between these two fuels also may have similar anchoring and mixing properties at $\varphi = 1$.

3.4. Syngas composition variation

The frequency at a given equivalence ratio shows a slight linear dependence on the hydrogen concentration as shown in Fig 6a. From this figure, it can be seen that with increasing hydrogen-content, the flame speed increases until a hard cutoff occurs, in which the instability is rendered inactive and the flame becomes non-resonating. The concentration at which this "quiet" limit occurs is equivalence ratio dependent, but the limit is extended for richer flames. Within

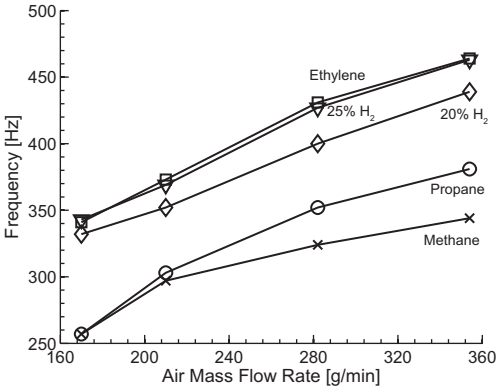

Fig. 5. Frequency of the instability as a function of the gas velocity, which is characterized by the air mass flow rate at $\varphi = 1.0$.

the range of equivalence ratios considered, the maximum cutoff occurs near 43% H_2. As well, this shift is quasi-stable for syngas, where once the flame is non-resonating, it will not transition back to resonating. Hydrocarbon fuels can display intermittent behavior where resonant transitioning can occur. As the "quiet" limit is approached, the instability strength is reduced until silent. This type of behavior suggests that thermoacoustic instabilities can be reduced by increasing the hydrogen content of the fuel. By also operating fuel-lean, the amount of hydrogen required to silence the flame is reduced. The data also implies that a critical combination of flame speed and shape/anchoring controls the acoustics for syngas.

3.5. Flame shape and Rayleigh criterion

Measurements showed that the intensity of the acoustic response was linked to the flame shape, and three distinct flame shapes could be identified (see Fig. 7b, d, and f). Specifically, it was observed that the instability was amplified when the flame had a flat disk-like shape (see Fig. 7f) that was slightly lifted. Flames that were directly anchored to the fuel annulus were generally non-resonating. Within the unstable resonating mode, two types of shape fluctuations were observed. The first type involved a flame liftoff height oscillation where the flame would move up or downstream. Steinberg et al. [13] have shown that the flame height oscillations are due piston-like pumping of the PVC and recirculation zones. The second motion was a change from a flat disk shape to a V-shape flame (see Fig. 7b), with varying degrees in between.

A Rayleigh index was calculated [28] for resonating and non-resonating syngas flames, and for a flat ethylene flame. For these indices, the pressure was recorded at a port located in the combustor wall, 1 cm above the injector face. Figure 7

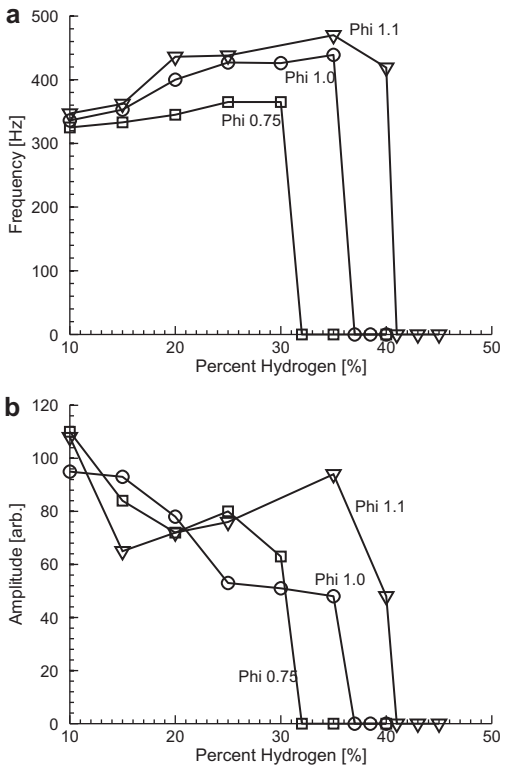

Fig. 6. (a) Frequency as a function of hydrogen composition, (b) amplitude as a function of hydrogen composition; for $m_a = 282$ g/min.

depicts the Rayleigh index field alongside chemiluminescence images of each respective flame. Rayleigh indices greater than zero represent thermo-acoustically amplified flames where the pressure field and heat release are in phase, thus satisfying the Rayleigh criterion. Indices less than zero represent dampening. Figures 7a and 7b show the flame profile for a non-resonating syngas flame. The index field is populated by values that are close to zero or slightly negative which is indicative of a field with little coupling between the pressure and heat release. Figures 7c and 7d display the same characteristics for a resonating flame and there exists a strong region of amplification surrounded by dampened regions, similar to that shown by Kang et al. [29]. Figures 7e and 7f depict a larger, lifted region of coupling for a flat ethylene flame. There are noticeable differences in the flame shapes between the resonating flames and the non-resonating syngas flame. The non-resonating syngas flame shows better anchoring and has an axially extended V-shape profile. While the resonating syngas flame is not as flat as the ethylene flame, its profile is wider at its base than the non-resonating syngas flame, which implies a higher degree of premixing. Flat flames are thermally compact and concentrate heat release in a smaller portion of the burner than an axially extended V-flame. Thus, V-flames are less effective at applying thermal energy toward acoustic amplification and satisfaction of the Rayleigh criterion.

3.6. Amplitudes of the oscillations

The amplitude behavior with equivalence ratio shows varying trends with each fuel, as seen in Fig. 8a. Propane shows a decrease in instability strength, while ethylene flames resonate more powerfully with increasing equivalence ratio. Both syngas mixtures show little variation in strength. These differences can be attributed to different flame shapes, Rayleigh indices, different oscillation frequencies, and different liftoff heights. It is evident that these behaviors are not all consistently scaled with the increase in global heat release.

The amplitude data for the syngas and the hydrocarbon fuels, as a function of mean flow velocity, are very different, as depicted in Fig 8b. While syngas drops in amplitude strength, thermoacoustic instabilities are amplified at higher flow rates for hydrocarbons. Ethylene proved to

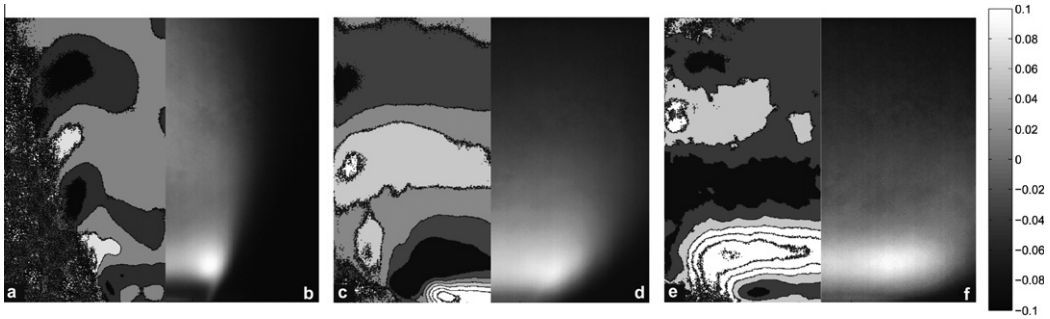

Fig. 7. Rayleigh index and chemiluminescence of syngas and ethylene flames for $\varphi = 0.75$, $m_a = 282$ g/min. (a and b) Non-resonating syngas flame, 40% H_2, 60% CO. (c and d) Unstable resonating syngas flame, 25% H_2, 75% CO. (e and f) Unstable resonating ethylene flame.

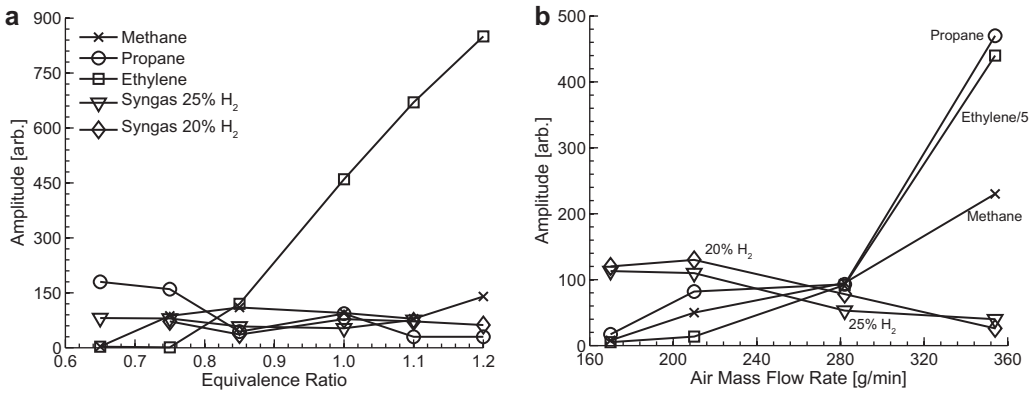

Fig. 8. Amplitude of the power spectrum peak. (a) Effect of varying equivalence ratio; for $m_a = 282$ g/min. (b) Effect of varying gas velocity for $\varphi = 1.0$. Ethylene amplitude data rescaled by a factor of five.

be significantly louder than all other fuels, as seen in Fig. 8b where it is rescaled by a factor of five. In comparison to hydrocarbons, the lift-off height is reduced for syngas mixtures. When this effect is combined with higher inlet velocities and the high diffusivity of hydrogen, reduced mixing can occur. The nominal flame shape is also different between the types of fuels presented. The hydrocarbon flames are typically observed to be flat, whereas the syngas flames have a wide V-shape, which tends to make them quieter.

4. Conclusion

The gas turbine model combustor exhibits a natural combustion instability, which creates a pressure spectrum that nominally has a single peak, but the frequency of this peak varied significantly, from 250 to 480 Hz, as the following operating parameters were varied: fuel type, flame speed, equivalence ratio, and air mass flow rate. A driven Helmholtz resonance is present. The geometry of the exhaust pipe and plenum greatly affected the acoustic frequency. Flame speed was found to play an important role since it affects the frequency and amplitude of the instability. Frequencies consistently increased with (and were highly correlated with) the burning velocity. The frequency also varied linearly with the average air flow velocity. This indicates that a convective–acoustic mechanism must depend on the flame liftoff height or some type of flashback oscillation, since flame speed should not affect the frequency of a pure Helmholtz resonator.

Syngas displayed different behavior than hydrocarbon fuels, even when the laminar flame speeds of the fuels were matched. This difference could be due to the lower molecular weight or Lewis number of the syngas, which affects the mixing, causing thermo-diffusive instabilities. A sufficient amount of hydrogen content in the syngas completely suppressed the instability. With increasing hydrogen-content in the syngas, the flame transitions from a lifted to a fully anchored flame, resulting in a drastic decrease in the acoustic amplitude. Thus, increasing the burning velocity causes two competing effects; the higher frequency oscillations compete with the tendency of the flame to anchor. Flame shape is important; when the flame was flat both the acoustic amplitude and the Rayleigh index were large, indicating that heat is released at a location that amplifies the instability. When V-flames occurred, the acoustic amplitude and the Rayleigh index were smaller. It is concluded that the instability is due to integrated-acoustics involving a combination of Helmholtz and convective–acoustic mechanisms, which are driven by flame speed effects.

Acknowledgments

This research was funded by ONR under Grant N00014-10-10561 and by the DOE-UTSR program under Grant FE0007060. The authors thank Dr. Wolfgang Meier of DLR Stuttgart for permission to use the GTMC design.

References

[1] N. Syred, *Prog. Energy Combust. Sci.* 32 (2) (2006) 93–161.
[2] J.W.S. Rayleigh, R. Lindsay, *The Theory of Sound* vol. 2, Dover Publications, 1945, p. 230.
[3] R. Giezendanner, P. Weigand, X.R. Duan, W. Meier, U. Meier, M. Aigner, *J. Eng. Gas Turb. Power* 127 (2005) 492–496.
[4] P. Weigand, W. Meier, X.R. Duan, W. Stricker, M. Aigner, *Combust. Flame* 144 (2006) 205–224.
[5] S. Ducruix, T. Schuller, D. Durox, S. Candel, *J. Propul. Power* 19 (5) (2003) 722–734.

[6] B.T. Zinn, T. Lieuwen, in: T. Lieuwen, V. Yang (Eds.), *Combustion Instabilities in Gas Turbine Engines*, AIAA, 2005, pp. 9–13.
[7] D. Rockwell, E. Naudascher, *J. Fluids Eng.* 100 (1978) 152–165.
[8] K.H. Yu, A. Trouvé, J.W. Daily, *J. Fluid Mech.* 232 (1991) 47–72.
[9] T. Lieuwen, H. Torres, C. Johnson, B.T. Zinn, *J. Eng. Gas Turb. Power* 123 (2001) 182–189.
[10] K. Zähringer, D. Durox, F. Lacas, *Int. J. Heat Mass Transfer* 46 (2003) 3529–3548.
[11] J.M. Samaniego, B. Yip, T. Poinsot, S. Candel, *Combust. Flame* 94 (1993) 363–380.
[12] S.K. Dhanuka, J.E. Temme, J.F. Driscoll, *Proc. Combust. Inst.* 33 (2011) 2961–2966.
[13] A.M. Steinberg, I. Boxx, M. Stöhr, C.D. Carter, W. Meier, *Combust. Flame* 157 (2010) 2250–2666.
[14] T. Lieuwen, V. McDonell, D. Santavicca, T. Sattelmayer, *Combust. Sci. Technol.* 180 (2008) 1169–1192.
[15] J. Fritz, M. Kroner, T. Sattelmayer, *J. Eng. Gas Turb. Power* 126 (2004) 276–283.
[16] O. Tuncer, S. Acharya, J.H. Uhm, *Int. J. Hydrogen Energy* 34 (2009) 496–506.
[17] W. Meier, X.R. Duan, P. Weigand, *Proc. Combust. Inst.* 30 (2005) 835–842.
[18] K. Kumar, G. Mittal, C.-J. Sung, C.K. Law, *Combust. Flame* 153 (2008) 343–354.
[19] C. Dong, Q. Zhou, Q. Zhao, Y. Zhang, T. Xu, S. Hui, *Fuel* 88 (2009) 1858–1863.
[20] R. Sadanandan, M. Stöhr, W. Meier, *Combust. Explos. Shock Waves* 45 (2009) 518–529.
[21] A.M. Steinberg, I. Boxx, M. Stöhr, W. Meier, C.D. Carter, *AIAA J.* 50 (4) (2012) 952–967.
[22] L.E. Kinsler, A.R. Frey, A.B. Coppens, J.V. Sanders, *Fundamentals of Acoustics*, John Wiley & Sons, Inc., 2000, p. 272.
[23] S.R. Chakravarthya, O.J. Shreenivasan, B. Boehm, A. Dreizler, J. Janicka, *J. Acoust. Soc. Am.* 122 (1) (2007) 120–127.
[24] A.P. Dowling, *J. Fluid Mech.* 394 (1999) 51–72.
[25] G.J. Bloxsidge, A.P. Dowling, P.J. Langhorne, *J. Fluid Mech.* 193 (1988) 445–473.
[26] T. Schuller, D. Durox, P. Palies, S. Candel, *Combust. Flame* 159 (2012) 1921–1931.
[27] G. Yu, C.K. Law, C.K. Wu, *Combust. Flame* 63 (1986) 339–347.
[28] W. Pun, S.L. Palm, F.E.C. Culick, *Combust. Sci. Technol.* 175 (2003) 499–521.
[29] D.M. Kang, F.E.C. Culick, A. Ratner, *Combust. Flame* 151 (2007) 412–425.